ZHONG TAO
GUO YUSEN
LIN LUYAO
and
LI DI

Research on rational staggered distance at combined mining face of contiguous coal seams with thinner top and thicker bottom and on relations between supports and wall rocks

For combined mining conditions of contiguous coal seams with thinner top and thicker bottom, the paper used overburden movement rules, stress superposition, and the theory of staggered distance as well to research on what influences the design of rational staggered distance at combined mining face and on relations between supports and wall rocks for the low seam face. The research results were: (1) through both overburden movement rules and stress superposition of coal seam roofs and floors, the paper computed staggered distances of contiguous coal seams, and the largest distance was determined as the correction value. The paper finally determined the rational staggered distance at combined mining face of contiguous coal seams to be 48 m. (2) In combination with the damage ranges of strata between rock layers and breakage intervals, the paper proposed an interbedded cantilever beam structure of "breakage blocks - loose blocks - damage blocks" that was formed on the overburden of the mined low seam face behind the stable-pressure area. (3) The paper analyzed the breakage height of the cantilever beam on the overburden and the roof control range. Computation results showed that the support resistance of the low seam face was 6000 KN.

Keywords: *Contiguous coal seams, combined mining, rational staggered distance, relations between supports and wall rocks.*

1. Introduction

Contiguous coal seams refer to those adjacent coal seams of ultra-close distance and with mutual effects during coal mining. With small layer distance, combined mining has long been a challenge in the field of mining engineering [1]. As outputs of coal mines continue to mount up, the difficulty in connecting working faces fails to guarantee normal coal mining outputs. Thus, it is of great practical significance to research on conditions of designing rational staggered distance at combined mining face of contiguous coal seams. Yang Wei et al. [2] considered the influence of stress distribution between rock layers. In combination with the influential scopes of support pressure at working faces, they used half plane body and mine pressure theory to have determined the fundamental conditions of designing staggered distance at working faces. Wei Lianyang et al. [3] pointed out that the overlying rock would undergo subsequent subsidence and caving twice, and that overburden caving would impact greatly on low seam mining. Ma Quanli [4] analyzed main influential factors of staggered distance, and computed the size of the low seam reduced-pressure zone and the minimum distance between the coal wall and the stable-pressure zone behind the up seam goaf. Through analysis, Sun Chundong et al. [5] concluded that under the conditions of combined mining of contiguous coal seams, locating working faces in reduced-pressure zones tended to cause interbedded fracture coalescence and even roof accidents. Thus, for combined mining of contiguous coal seams, in order to ensure safe production at the low seam face, and to prevent the low seam from continuous impact of mining subsidence, the research in the paper was emphasized on locating low seam face in stable-pressure zones.

2. Geological conditions and production technology of the working faces

The mining work was conducted in two working faces of a certain coal mine, namely II_1-11070 and II_3-11070, whose average elevation was -520 m and average distance from each other was 8 m. The stratigraphy of coal seam roof and floor is shown in Fig.1 as follows. For II_1-11070, the mean coal seam thickness was 6.2 m, and the mean tilt angle was 25°. We adopted the caving technique of "mining once and caving once" and "single-round ascending sequence" by mining 2.5 m and caving 3.7 m in a single round. For II_3-11070, the mean

Messrs. Zhong Tao, Guo Yusen and Lin Luyao, Faculty of Resource Engineering, Longyan University, Longyan, Fujian, 364 012, Zhong Tao, Guo Yusen and Lin Luyao, Longyan Mining and Safety Engineering Research Center, Longyan, Fujian, 364 012, Li Di, Changchun Gold Design Institute, Changchun, Jilin, 130 000, China. Email: zhongtao@lyun.edu.cn

coal seam thickness was 1.5 m, and the mean tilt angle was 25°. We adopted the backward full-mechanized caving mining method by advancing the working faces at the rate of 4.8 m/d. The staggered layout of mining roadways presented itself as a large spreading face. The mining roadway of II_1-11070's working face was underneath the solid coals of II_3-11070, and the mining roadway of II_3-11070's working face was underneath the goaf of II_3-11070's working face (Fig.2).

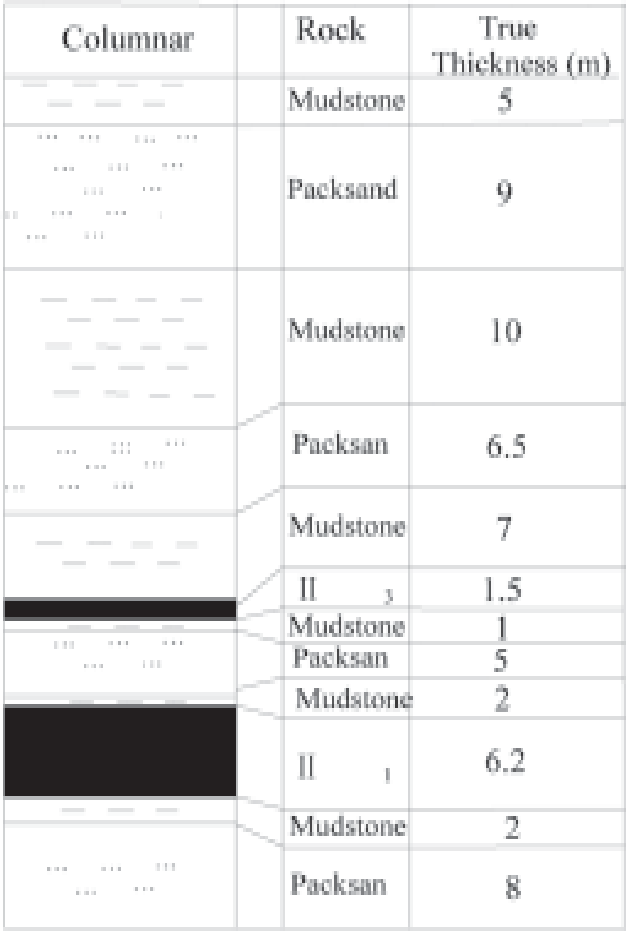

Fig.1 Stratigraphy of coal seam roof and floor

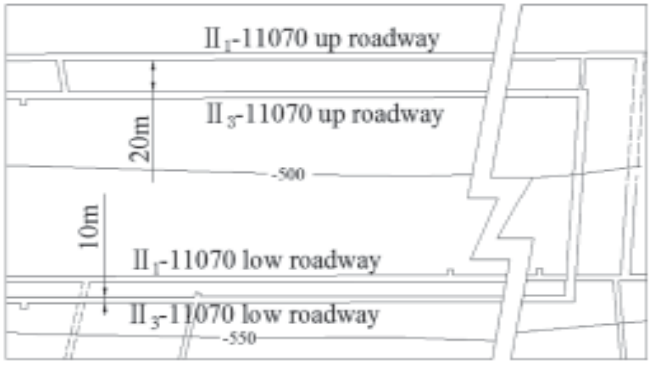

Fig.2 Mining roadway layout plan

3. Influential factors and computation of staggered distance at working faces

When determining the rational staggered distance at working faces, we should avoid the low seam face to be under the state of stress concentration lest it should affect safe and effective production at working faces. The primary effect factors of staggered distance contained stress concentration in strata between rock layers, up seam roof caving impact, and lead abutment pressure of low seam mining [6-8]. When determining staggered distance at working faces, it should be ensured that both the margin of stress concentration areas on the 5-meter fine sandstone between rock layers and the caving impact point on the 6.5-meter fine sandstone at the up seam should exceed the peak point of lead abutment pressure at the low seam face, and the larger excess value was determined as the correction value of the influential factors [9]. In strata between rock layers, taking the 5-meter fine sandstone as the major support layer of the overburden load would impact on mining pressure behaviors at the low seam face at the same time, thus it should be avoided to superpose up area stress and low area stress.

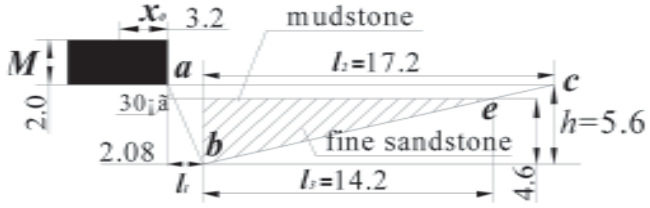

Fig.3 Stress concentration areas of fine sandstone between rock layers

3.1 Stress concentration areas of strata between rock layers

Up seam mining led to production of stress concentration in the goaf floor stratum. In Figure 3, the abc broken line denotedd the floor slippage boundary, and the shadow region denotedd the stress concentration areas of fine sandstone between rock layers. Then, the vertical depth h of goaf floor breakage, the vertical distance l1 from the coal wall, and the breakage length l2 of the advanced direction were expressed respectively as:

$$h = \frac{x_0 \cos\varphi_f}{2\cos\left(\frac{\varphi_f}{2}+\frac{\prod}{4}\right)} e^{\left(\frac{\varphi_f}{2}+\frac{\prod}{4}\right)\tan\varphi_f}$$

$$l_1 = \tan 30^o h$$

$$l_2 = x_0 \tan\left(\frac{\varphi_f}{2}+\frac{\prod}{2}\right) e^{\frac{\prod}{2}\tan\varphi_f}$$

where, $x_0 = \frac{M}{2\xi\tan\varphi}\ln\frac{2\gamma H + C\cot\varphi}{\xi C\cot\varphi}$, M - the maximum coal seam depth, 2.0 m; ξ - the triaxial stress coefficient,

; k - the maximum stress concentration coefficient, 2.0; γ - the average volume weight of the overburden, 24 KN/m^3; H - the average depth of the working face, 520 m; C - internal cohesion force of the coal, 0.8 MPa; - internal friction angle of the coal, 16°; f - friction coefficient between coal seam and the floor, ; φ_f - internal friction angle of the strata between rock layers, 32°.

After the coefficient values were substituted into the above expressions, it could be obtained that h = 5.6 m, l_1 = 3.2 m, l_2 = 17.2 m, and l_3 = 14.2 m. Thus, the length of the stress concentration area of fine sandstone was $L_1 = l_1 + l_3$ = 3.2+14.2 = 17.4 m.

3.2 Distance from the dynamic loading impact point of the main roof

When seam caving happened, certain dynamic impact and stress concentration against floor stratum would arise from the end of the 6.5-meter fine sandstone main roof at the up seam face [10]. Stress superposition, if happening, would threaten low seam face production, thus the paper computed periodical caving distance of the up seam roof. As the up seam main roof was 6.5-meter fine sandstone, the safe rock beam span method was used to compute caving distance. Take the safety factor n = 4 [11], then the safe span of the roof stratum was computed as:

$$l_4 = \frac{1}{1+\sin\varphi}\sqrt{\frac{7.2\times10^6}{6.5\times\sqrt{3}\times4\times0.24\times10^6}} = 10.2$$

where h - the 6.5-meter fine sandstone of the main roof; R_T - extreme tensile strength of the fine sandstone, 10.5 MPa; q - loading of the 6.5-meter fine sandstone, 0.24 MPa.

Meanwhile, according to the support type of the working faces, the maximum roof control distance was l_5 = 4.3 m. Thus, the distance of the impact point from the coal wall was $L_2 = l_4 + l_5$ = 4.3+10.2 = 14.5 m.

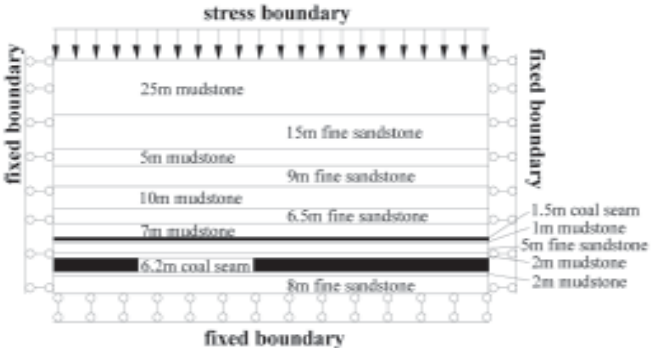

Fig.4 Scheme model diagram

3.3 The scope of advanced support pressure in full-mechanized working faces of the low coal seam

The model was established according to stratigraphy of coal seam roof and floor in Fig.1. The physical and mechanical parameters referred to Table 1. The model length was designed as 200 m. Horizontally, each 30-meter boundary coal pillar was designed to stand at the right side and the left sides so as to reduce impacts on boundaries. The model had 14 layers in total. The corrected model height was 103.2 m, and the lithological characters and height of various layers were seen in Fig.4. The full up seam was mined at the cyclic footage of 3.0 m, while the low coal seam was mined by top coal caving. The mechanized height was 2.5 m, and the top-coal caving height was 3.7 m. Solve function was adopted to realize model balance.

Fig.5 shows the lead abutment pressure distribution curves during low coal seam mining under the stable-pressure zone. The measured curve was placed on the contact surface between the 5-meter fine sandstone and the 2-meter mudstone at a 1-meter distance between measuring points. The seam thicknesses were 4 m, 6.2 m and 8 m, respectively, denoting the minimal seam thickness, the average one, and the maximal one. Fig.5 shows that the stable pressure behind the low seam goaf is 9.5 MPa, influencing a maximal length of 18 m. Thus, the influential length of the lead abutment pressure was defined as L_3 = 18 m.

Table 1: Physical and mechanical parameters of the coal and rock mass

Number	Lithology	Bulk modulus / GPa	Shear modulus / GPa	Bulk density / N.m^{-3}	Friction angle / °	Cohesion / MPa	Tensile strength / MPa
11	Fine sandstone	15	7.5	26500	31	15.7	7.2
10	Mudstone	11.7	5.4	25500	29	5.5	2.8
9	Fine sandstone	15	7.5	26500	31	15.7	7.2
8	Mudstone	10.5	4.52	25500	29	5.5	2.8
7	II$_3$ coal	5.91	2.5	14000	20	1	0.2
6	Mudstone	10.5	4.5	25500	29	5.5	2.8
5	Fine sandstone	15	7.5	26500	31	15.7	7.2
4	Mudstone	10.5	5.4	25500	29	5.5	2.8
3	?1 coal	5.91	2.5	14000	20	1	0.2
2	Mudstone	10.5	5.4	25500	29	5.5	2.8
1	Fine sandstone	15	8	26500	31	15.7	7.2

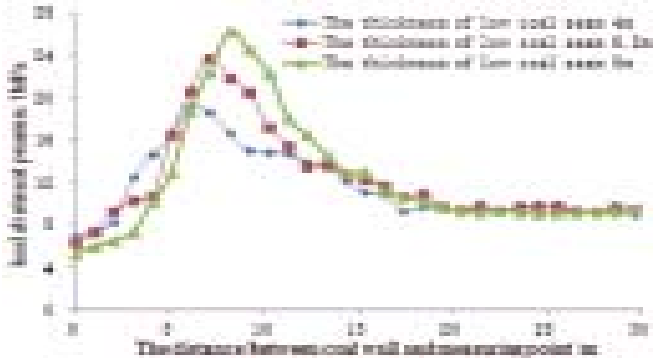

Fig.5 The lead abutment pressure distribution curves during low seam mining

4. Computation of rational staggered distance at working faces

For stress concentration of strata between layers which was resulted from up seam mining, the larger value should be chosen between the impact point distance (14.5 m) of main roof dynamic loading and the stress concentration area (17.4 m) that was formed when the seam floor was broken. Therefore, the length of the stress concentration area of up coal seam was 17.4 m, and the influential length of the lead abutment pressure of low seam roof was L_3 = 18 m.

According to the analysis of the influential factors of up seam and low seam, the equation of the rational staggered distance at working faces was given as:

$$L = L_1 + L_3 + C = 17.4+18+10 = 45.4 \text{ m}$$

where C denoted the safe distance, which was generally equal to or large than 10 m [12]. The paper hence defined the safe distance as the minimal value of 10 m. Through computation, the staggered distance was 45.4 m. Considering on-site production, the corrected staggered distance was 45 m.

5. Research on the relations between the support and the wall rock of the full-mechanized working face of the low seam

As the final staggered distance was 45 m, low seam mining was undertaken when the up seam was exploited stably, whose overburden movement rule was different from general full-mechanized working faces. As there existed loose blocks and breaking articulated blocks over the strata between layers, based on the traditional relations between the support and the wall rock of the full-mechanized working face of the low seam, and in combination with the damage areas and breakage intervals of the strata between layers, the paper proposed the interbedded "support – breaking block – loose block – damage block" cantilever beam structure that was formed on the overburden of working faces under the stable-pressure zone during combined mining of contiguous coal seams [13-14].

The four zones that were divided by red lines in Fig.6 is the areas where overburden impacted on supports.? denoted the friction angle of strata, being defined as 20°in the paper.

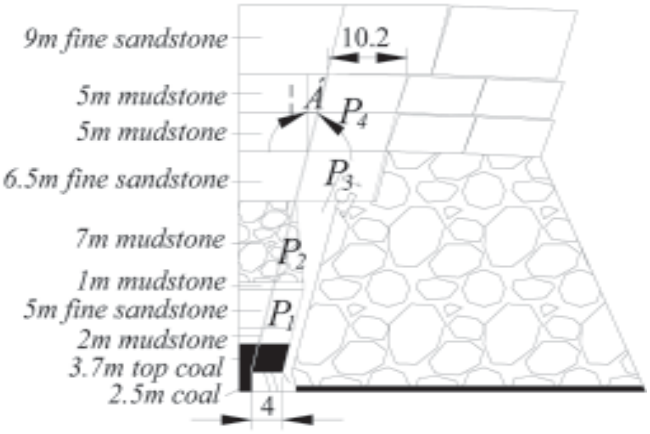

Fig.6 The relation diagram between the support and the wall rock of low coal seam

TABLE 2: PARAMETER COMPUTATION OF OVERBURDEN LOAD

Number	Rock mass	Density	Thickness / m	Coefficient of bulk increase bulking coefficient	Suspension girder length / m	Range	Load / KN/m
11	Fine sandstone	2500	9	-	-	-	-
10	Mudstone	2400	10	0.2	10.2	P4	734.4
9	Fine sandstone	2500	6.5	0.3	10.2	P3	1657.5
8	Mudstone	2400	7	0.3	2	P2	336
7	Coal	1400	1.5	-	-	-	-
6	Mudstone	2400	1	0.2	4	P1	96
5	Fine sandstone	2500	5	0.3	4	P1	500
4	Mudstone	2400	2	0.25	4	P1	192
3	Top coal	1400	3.7	-	4	P1	207.2
2	Coal	1400	2.5	-	-	-	-
Sum	-		-	-	-	-	3723.1

The effective roof control distance of the support was 4 m. P_1 corresponds to the damage area of coal and rock mass. The 1-meter mudstone and 5-meter fine sandstone were damage areas of up seam floor. The 2-meter mudstone and the 3.7-meter roof coal were damage areas of repeating support. P_2 corresponded to the loose block area. As the area was at the loose state, the angle of repose and the fracture angle of the rock layer were in the opposite direction. P_3 corresponded to the breaking block area, whose caving interval was 10.2 m. P_4 corresponded to the articulating area that generates additional loading. The roof caving height was computed according to the expression of $h = \frac{M}{K=1}$, where M denoted the equivalent height of the coal seam [15]. According to the coal mine operational rules, the mining rate of mechanized coal and top-coal should be equal to or large than 97 % and 93 %, respectively. Thus M was defined as 7.2 m.

As the corresponding caving height covered the 10-meter mudstone, the loading could not be computed at the value of 10 m. P_1~P_3 was computed according to the volume weight of the rock mass. The additional load of P_4 was computed at 0.3 time volume weight of the 10-meter mudstone. Articulated structures that arised both in P_4 and the 9-meter fine sandstone protected the face pressure behavior. Considering safety factors, when computing working pressure of the working face support, it should be considered that the most perilous condition was when point contact was forming between P_2 and P_3 while P_3 was with articulating structure, namely that the up margin point of the bulking space of the 7-meter mudstone contacted the 6.5-meter fine sandstone. This situation would not occur in on-site coal production, as before point contact was forming between P_2 and P_3, P_3 (6.5-meter fine sandstone) realized caving. Thus there was larger safe remainder for working resistance of supports than that for on-site face pressure.

The per-unit-length load of the working face support towards the tilting direction was 3723.1 KN/m. According to the fact that the existing width of all top-coal supports was 1.5m, the computed rated working resistance of the support was 3723.1×1.5=5585 KN. Hence the rated working resistance of the chosen support was no less than 5585 KN. In combination with on-site situations, ZF6000/18/28 was chosen as the support type in the paper.

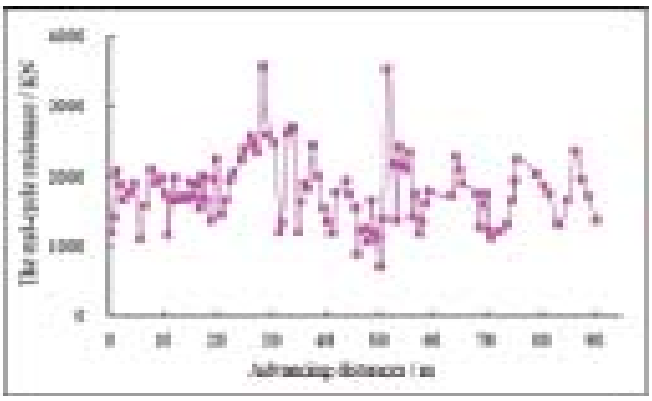

Fig.7 The relation between the end-cycle resistance and the advancing distances of working faces

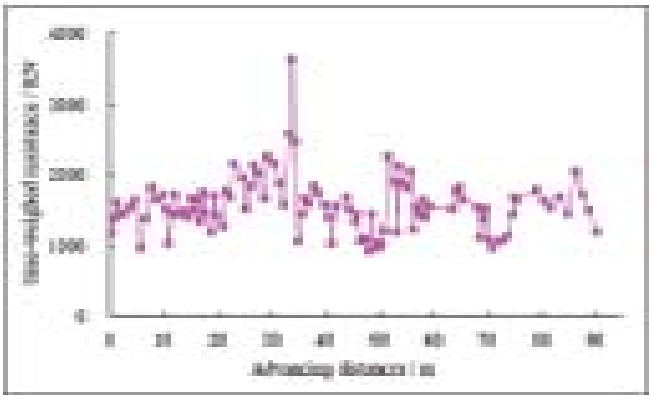

Fig.8 The relation between the time-weighed resistance and the advancing distances of working faces

TABLE 3: ROOF WEIGHING CHARACTERISTICS IN THE MIDDLE OF THE FULL-MECHANIZED II_1-11070 WORKING FACES

Interval / m	Weighing term / kN		Non-weighing / kN		Dynamic loading coefficients	
	Pm	Pt	Pm	Pt	Km	Kt
9.2	2612.0	2056.1	2083.5	1976.0	1.25	1.04
7.2	2672.0	2084.3	2104.5	2008.3	1.25	1.04
8.7	2520.0	1731.7	1896.8	1680.1	1.33	1.03
7.6	2688.0	1956.5	2069.7	1923.0	1.30	1.02
7.0	2543.5	1846.2	1967.4	1846.2	1.30	1.02
7.8	2778.0	2014.7	2218.1	1918.6	1.25	1.05
8.0	2893.5	2023.6	2272.1	2007.2	1.27	1.01
7.9	2678.4	1991.3	2091.9	1918.7	1.28	1.04

6. Measurement analysis of working face pressure

During combined mining of the working faces, the rational staggered distance of the working faces was defined as 45m. There was a total of 106 supports along the working faces. Fig.7 and Fig.8 show the relations between the end-cycle resistance and time-weighed resistance of the 52# support in the middle of II_1-11070 working faces and the advancing distances of the working faces.

Among the analyzed measurement data, there were totally six weighing times for 52# support, with the initial weighing interval of 28.7 m; the maximal periodical weighing interval was 13.7m, and the minimal one was 9.2 m, with the average value of 11.5 m; during the weighing term, the average end-cycle resistance and the average time-weighted resistance were 2678.4 kN and 1991.3 kN, respectively, accounting for

44.64 % and 33.19 % of the rated working resistance?during the non-weighing term, the average end-cycle resistance and the average time-weighted resistance were 2091.9 kN and 1918.7 kN, respectively, accounting for 34.87 % and 31.98 % of the rated working resistance; the dynamic loading coefficients during the weighing term were: Km=1.28, and Kt=1.04. It showed that during weighing terms, there were apparent static loading characteristics for supports, and that there were small dynamic loading and smooth weighing as well; It showed that if the staggered distance of combined mining at working faces was 45 m, the pressure behavior at low seam face would be reduced to such a degree that there was no large-scale high-strength weighing. At the same time, there was large safety remainder in the face supports, which ensured safe production. It showed that if the staggered distance of combined mining at working faces was 54m, there would be smooth pressure at the low seam face without large stress concentration and strong pressure behavior, which ensured safe production.

7. Conclusions

(1) The staggered distance is computed on the basis of both the overburden movement rule and stress concentration at the seam roofs and floors, and the larger value is determined as the correction value. Meanwhile, considering the impact of lead abutment pressure at the low seam, the paper finally chooses the rational staggered distance of the combined mining at the working faces as 45 m.

(2) In combination with the damage areas and breakage intervals of the strata between layers, the paper proposes the interbedded cantilever beam structure of "supports – breakage blocks – loose blocks – damage blocks", and also identifies the four structural characteristics partitions.

(3) The paper analyzes the fracture height of the overburden cantilever beam and the roof control scopes, and obtains that the support resistance of the low seam face support is 6000 KN through computation. On-site results show that there are apparent static loading characteristics for low seam face supports, and that the effective working state realizes safe and efficient mining, which also proves the rationality of defining the staggered distance of combined mining at working faces to be 45 m.

Foundation items

1. Hundreds of Longyan University young teachers climbing project (LQ2015036)
2. Longyan science and technology plan projects (2014LY33)

References

1. Kang, J., Sun, G. Y. and Dong, C. J. (2010): "Overlying Strata Movement Law of Ultra-Close Thin Coal Seam Adopting Simultaneous Mining Face." *Journal of Mining & Safety Engineering*, 27(1): 51-56.
2. Yang, W., Liu, C. Y., Huang, B. X. and Yang, Y. (2012): "Determination on Reasonable Malposition of Combined Mining in Close-Distance Coal Seams." *Journal of Mining & Safety Engineering*, 29(1): 101-105.
3. Wei, L. Y. (2009): "Research on the reasonable distance when the close seams joint." *Hebei Coal*, 35(6): 11-12.
4. Ma, Q. L., Geng, X. W. and Tong, P. G. (2006): "Reasonable Malposition Setting in Close Distance Coal Seams Simultaneous Mining Working Face." *Coal Engineering*, 11-13.
5. Sun, C. D., Yang, B. S. and Liu, C. (2011): "Strata behavior regularity of 1.0 m very contiguous seams combined mining." *Journal of China Coal Society*, 36(9): 1423-1428.
6. Li, H. X., Li, B. and Bai, X. (2015): "Three Dimensional Modeling of Gas-Solid Coupled Free And Porous Flow In A Filtration Process." *International Journal of Heat and Technology*, 33(4): 101-106.
7. Huang, X., Wang, C., Wang, T. and Zhang, Z. (2015): "Quantification of Geological Strength Index Based on Discontinuity Volume Density of Rock Masses." *International Journal of Heat and Technology*, 33(4): 255-261.
8. Liu, J., Liu, Z., Wang, S., Shi, C. and Li, Y. (2016): "Analysis of microseismic activity in rock mass controlled by fault in deep metal mine." *International Journal of Mining Science and Technology*, 26(2): 235-239.
9. Cao, S., Song, W., Deng, D., Lei, Y. and Lan, J. (2016): "Numerical simulation of land subsidence and verification of its character for an iron mine using sublevel caving." *International Journal of Mining Science and Technology*, 26(2): 327-332.
10. Yan, G. C., Hu, Y. Q., Song, X. M., Fu, Y. P., Liu, Z. H. and Yang, Y. (2009): "Theory and physical simulation of conventional staggered distance during combined mining of ultra-close thin coal seam group." *Chinese Journal of Rock Mechanics and Engineering*, 28(3): 591-597.
11. Yang, W., Liu, C. Y. and Yang, Y. (2012): "Reasonable Malposition Setting in Close Distance Coal Seams under Influence of Interlaminar Stresses." *Chinese Journal of Rock Mechanics and Engineering*, 31(1): 2965-2972.
12. Tian, C. S., Bai, Z. F. and Qu, X. X. (2006): "Character of Overlying Strata Structure for Fully Mechanized Coal Face with Sublevel Caving in Lower-slicing." *Journal of Henan Polytechnic University*, 25(3): 191-195.
13. Christopher, M. (2016): "Coal bursts in the deep longwall mines of the United States." *International Journal of Coal Science & Technology*, 3(1): 1-9.
14. Ryszard, H. (2015): "Modelling of time dependent subsidence for coal and ore deposits." *International Journal of Coal Science & Technology*, 2(4): 287-292.
15. Gong, H. P., Li, J. W. and Chen, B. B. (2013): "Overlying Strata Structure and Surrounding Rock Stability of Mining Near-distance Coalseams." *Coal Mining Technology*, 11(5): 90-92.